

Evaluation of Luenberger Observer Based Sensorless Method for IM

Vladimir M. Popovic, Marko A. Gecic, Veran V. Vasic, Djura V. Oros, Darko P. Marcetic

Faculty of Technical Science

Novi Sad, Serbia

Abstract—System approach for analysis of Luenberger observer for vector-controlled induction motor drives without shaft sensor is presented in this paper. Important aspects of control algorithm for induction motor system were described in detail. Realization of control algorithm based on Luenberger observer calculation method for estimation of unknown induction motor states is performed within appropriate digital signal controller (DSC). Verification is given through simulation and experimental results of vector-controlled induction motor sensorless drive.

Keywords—vector control; Luenberger observer, induction motor

NOMENCLATURE

\mathbf{u}_s	– stator voltage vector
\mathbf{i}_s	– stator current vector
$\boldsymbol{\psi}_r$	– rotor flux vector
R_s	– stator phase resistance
R_r	– rotor phase resistance
L_m	– mutual inductance
L_r	– rotor self inductance
T_r	– rotor circuit time constant
L_σ	– equivalent stator circuit leakage inductance
ω_r [rpm]	– actual rotor angular speed
T_e	– electromagnetic torque
T_m	– load torque
J_m	– motor inertia coefficient
P	– number of motor pole pairs

I. INTRODUCTION

Various methods based on sensorless vector control (VU) of induction motor (IM) drives have been studied and proposed over past few decades, [1–6]. One of the very versatile techniques based on observer characteristic, [3–6], are in advantage to open-loop techniques, [1] and [2], because of feedback control law inherited within observation phenomena.

Digital signal controller (DSC) based IM vector-controlled drives without shaft sensor in very first period of their exploitation were exclusively used for low performance drive applications. Specified algorithms for estimation of unknown machine states are demanded in the case of VU *sensorless* drives and such algorithms could only be implemented in high-speed DSC platforms. Concept of VU for performance improvements of these drives also requires the use of power electronic devices with high frequency switching capabilities. Stability and robustness of vector-controlled *sensorless* drives are crucial attributes for quality drive operation. For the fulfillment of these conditions the use of quality and often expensive micro- and power-electronic devices is imposing as inevitable fact.

Today, with the grown-up trend of development and price reduction in area of electronics goes the increase in the use of *sensorless* VU drives. More complex and sophisticated control algorithms can be transferred to DSC and high performance characteristics of IM drives can be achieved. This enables the utilization of these drives in high performance drive applications. Lack of shaft sensor leads to decrease in cost and the increase in reliability and security of considered drives. Complicated installation of optical incremental encoder or resolver cables and connectors magnifies the risks of various faults. Besides, mounting of a shaft sensor is not applicable in many areas of practical usage, [9].

Global needs for power efficiency often impose the utilization of specified algorithms within control unit for better evaluation of IM states. One of the most common used algorithms for estimation and improvement in control performance of IM drive is based on mathematical model of IM called Luenberger observer (LO). In this paper, evaluation of LO based *sensorless* method for IM, theoretical introduction in system observability as well as the construction method for appropriate LO and DSC realization are considered. Validation is given through simulation and experimental results at various operational conditions.

II. INTRODUCTION TO OBSERVERS

The availability of entire state vector is essential for performance improvement of general system S governed by

$$\dot{\mathbf{x}}(t) = \mathbf{A}\mathbf{x}(t) + \mathbf{B}\mathbf{u}(t). \quad (1)$$

Optimal control law implementation in form of

$$\mathbf{u}(t) = \boldsymbol{\varphi}(\mathbf{x}(t), t), \quad (2)$$

can be constructed for relevant system S if its entire state vector is known e.g. through measurement. In practice this differs for the most of complex systems where some items within state vector remain unknown because of measurement disability nature of corresponded items. In that case, one of the most common approach for construction of control law deduced in form of (2) includes the estimation of unknown part of state vector in the manner of system observability phenomena.

System observability characteristic involves the fact of linear tracking the state vector of supervised system S_1 via state vector of second system S_2 which is, in the most cases, driven by available outputs of system S_1 . Such driven system is called the observer to S_1 system. As a result, unknown part of the S_1 state vector can be derived for control law implementation or other *sensorless* control methods within general system.

Here, free observation system theorem will be introduced for better understanding of a system observability characteristic. Further theoretical analysis will be restricted to linear time-invariant systems without of loss in generality.

Theorem 1: Let S_1 be a free system, $\dot{\mathbf{x}}(t) = \mathbf{A}\mathbf{x}(t)$, which drives S_2 $\dot{\mathbf{z}}(t) = \mathbf{F}\mathbf{z}(t) + \mathbf{H}\mathbf{x}(t)$. Suppose there is a transformation \mathbf{T} which satisfy $\mathbf{T}\mathbf{A} - \mathbf{F}\mathbf{T} = \mathbf{H}$. If $\mathbf{z}(0) = \mathbf{T}\mathbf{x}(0)$, then $\mathbf{z}(t) = \mathbf{T}\mathbf{x}(t)$ for all $t \geq 0$. Or more generally,

$$\dot{\mathbf{z}}(t) = \mathbf{T}\dot{\mathbf{x}}(t) + e^{\mathbf{F}t}[\mathbf{z}(0) - \mathbf{T}\mathbf{x}(0)]. \quad (3)$$

Proof: We may write immediately

$$\dot{\mathbf{z}}(t) - \mathbf{T}\dot{\mathbf{x}}(t) = \mathbf{F}\mathbf{z}(t) + \mathbf{H}\mathbf{x}(t) - \mathbf{T}\mathbf{A}\mathbf{x}(t). \quad (4)$$

Substituting $\mathbf{T}\mathbf{A} - \mathbf{F}\mathbf{T} = \mathbf{H}$ this becomes

$$\dot{\mathbf{z}}(t) - \mathbf{T}\dot{\mathbf{x}}(t) = \mathbf{F}[\mathbf{z}(t) - \mathbf{T}\mathbf{x}(t)] \quad (5)$$

which has (3) as a solution, [7].

One of the most convenient observer is one where transformation matrix \mathbf{T} is the identity matrix \mathbf{I} ($\mathbf{T} = \mathbf{I}$). This observer is called the identity observer because state vector of free system $\mathbf{x}(t)$ is identically related to the observer state vector $\mathbf{z}(t)$ as shown in the form

$$\mathbf{z}(t) = \mathbf{x}(t). \quad (6)$$

As a result, those systems have same dynamic order. Thus, specification of the observer rest on the specification of matrix \mathbf{H} . Again, if we consider observer system S_2 in altered form deduced as

$$\dot{\mathbf{z}}(t) = \mathbf{F}\mathbf{z}(t) + \mathbf{G}\mathbf{y}(t), \quad (7)$$

where $\mathbf{y}(t)$ is available (often through measurement) part of system state vector $\mathbf{x}(t)$

$$\mathbf{y}(t) = \mathbf{C}\mathbf{x}(t), \quad (8)$$

with constant matrix \mathbf{C} , under the assumption of identity transformation employment within observation system, the same observation system can be written in form of

$$\dot{\mathbf{z}}(t) = (\mathbf{A} - \mathbf{G}\mathbf{C})\mathbf{z}(t) + \mathbf{G}\mathbf{y}(t). \quad (9)$$

Any matrix \mathbf{G} leads to the observer system but the estimation dynamic of observer depends on the selection of matrix \mathbf{G} coefficients. For stable observation of unknown system state, eigen-values of observer system matrix (poles of observer) are often allocated to be proportionally negative semi-definite according to roots of free system. Convergence dynamic within observation of a free system state vector is upgraded and as a result, state vector of system is available for the purposes of e.g. control improvements in a form of optimal control law (2), [7].

III. MATHEMATICAL MODELS OF INDUCTION MOTOR AND LUNEBERGER OBSERVER

LO belongs into category of deterministic observers because it is based on mathematical model of considered system. Base goal in this section is to describe the construction of LO for unknown states and rotor speed observation of IM in a purpose of performance improvements of IM *sensorless* drive.

A. Mathematical model of induction motor

Mathematical model of IM in stationary reference $\alpha\beta$ frame with stator current and rotor flux vectors as IM state vector is suitable for VU concept development. It is presented in extended matrix form as

$$\begin{bmatrix} \dot{\mathbf{i}}_s \\ \dot{\boldsymbol{\psi}}_r \end{bmatrix} = \begin{bmatrix} -(R_s + \frac{R_r L_m^2}{L_r^2})/L_\sigma & -(\frac{L_m}{L_\sigma L_r})(-1/T_r + j\omega_r) \\ L_m/T_r & (-1/T_r + j\omega_r) \end{bmatrix} \begin{bmatrix} \mathbf{i}_s \\ \boldsymbol{\psi}_r \end{bmatrix} + \frac{1}{L_\sigma} \begin{bmatrix} \mathbf{u}_s \\ \mathbf{0} \end{bmatrix}. \quad (10)$$

which has a simplified form in state space as presented in (1), [8].

Stator current vector is also a measurable vector and as a part of IM state vector it can be written in shortened matrix form as

$$\mathbf{i}_s(t) = \mathbf{C}\mathbf{x}(t), \quad (11)$$

where $\mathbf{C} = [\mathbf{I} \ \mathbf{0}]$ is 2×4 dimension constant matrix.

Electromagnetic torque of IM in a form of vector equation is considered by

$$T_e = \frac{3}{2} p \frac{L_m}{L_r} (\boldsymbol{\psi}_r \times \mathbf{i}_s). \quad (12)$$

Complete mathematical model of IM is enclosed by adding the mechanical system differential equation which describes mechanical phenomena in IM. This is governed by

$$T_e - T_m = J_m \frac{d}{dt} \omega_m, \quad [8]. \quad (13)$$

B. Mathematical model of Luenberger observer

According to the IM model attributes, complete model of LO for IM state observation in shortened matrix form is given as

$$\dot{\hat{\mathbf{x}}}(t) = \hat{\mathbf{A}}\hat{\mathbf{x}}(t) + \mathbf{B}\mathbf{u}(t) + \mathbf{G}(\hat{\mathbf{i}}_s - \mathbf{i}_s), \quad (14)$$

where variables with $\hat{}$ represents observed variables from LO and matrices $\hat{\mathbf{A}}$ and \mathbf{B} represents LO system and LO control matrices with 4×4 and 4×2 dimension rate, respectively. It should be advised that, in general, those matrices do not have to fit in original to corresponding IM system matrices.

It is shown in section II that the construction of LO observer when the system model is known rest on definition of matrix \mathbf{G} , so called feedback action matrix. This matrix is multiplied with the stator current error vector and in summary, this has affect in the decrease in estimation error due to the mismatch in rotor speed or parameters values within IM and LO models. It is given in a form of

$$\mathbf{G} = \begin{bmatrix} g_1 \mathbf{I} + g_2 \mathbf{J} \\ g_3 \mathbf{I} + g_4 \mathbf{J} \end{bmatrix}, \mathbf{I} = \begin{bmatrix} 1 & 0 \\ 0 & 1 \end{bmatrix}, \mathbf{J} = \begin{bmatrix} 0 & -1 \\ 1 & 0 \end{bmatrix}, \quad (15)$$

where g_1, g_2, g_3 and g_4 are coefficients of matrix \mathbf{G} .

In practice, the most common approach for designing the observer is to place the eigen-values of LO system matrix $\boldsymbol{\lambda}_0$ in proportional negative semi-definite correlation due to the roots of IM system matrix $\boldsymbol{\lambda}$ where IM is a stable system for itself. In [5] it is proven that gain selection of matrix \mathbf{G} which constitutes the observer system matrix has an influence on convergence dynamic of IM states. For stable and more robust estimation, matrix gains are chosen in a way of

$$\lambda_0 = k\lambda, \quad (16)$$

where k is coefficient of proportionality of IM and LO system poles.

Due to the previous, matrix G gains are derived as

$$g_1 = -(k-1)(\alpha + 1/T_r) \quad (17)$$

$$g_2 = (k-1)\hat{\omega}_r \quad (18)$$

$$g_3 = -(k^2-1)(\alpha/\beta + \gamma) + 1/\beta(k-1)(\alpha + 1/T_r) \quad (19)$$

$$g_4 = -1/\beta \cdot (k-1)\hat{\omega}_r \quad (20)$$

where $\alpha = (R_s + L_m^2/(L_r T_r))/L_\sigma$, $\beta = L_m/(L_r L_\sigma)$ and $\gamma = L_m/T_r$, [5].

Classical version of LO for IM drive assumes that the rotor speed is a variable parameter. In the essence of *sensorless* IM drives lies the Lyapunov function candidate governed by

$$V(\mathbf{e}) = \mathbf{e}^T \mathbf{e} + \frac{(\hat{\omega}_r - \omega_r)^2}{\lambda}, \quad (21)$$

where \mathbf{e} represent error estimation vector and λ is a positive constant, [5].

If LO system matrix eigen-values are negative semi-definite the proposed estimation algorithm will be asymptotically stable. Based on the equalization of first derivative of this criterion function with zero

$$\begin{aligned} \frac{dV(\mathbf{e})}{dt} &= \mathbf{e}^T [(\mathbf{A} + \mathbf{GC})^T + (\mathbf{A} + \mathbf{GC})] \mathbf{e} - \hat{\mathbf{x}}^T \Delta \mathbf{A}^T \mathbf{e} - \mathbf{e}^T \Delta \mathbf{A} \hat{\mathbf{x}} + \\ \frac{2\Delta\omega}{\lambda} \frac{d\hat{\omega}_r}{dt} &= 0, \end{aligned} \quad (22)$$

proposed speed observation is maintained when the sum of second, third and fourth term of the right side of (22) equals to zero.

Solution of previous determines the adaptive mechanism for rotor speed estimation governed by

$$\hat{\omega}_r = \int_c^\lambda (\hat{\psi}_{\beta r} e_{i\alpha s} - \hat{\psi}_{\alpha r} e_{i\beta s}) dt \quad (23)$$

where $c = L_\sigma L_r / L_m$, [5].

Thus, IM system is linearized and for better dynamic response of observed rotor speed, proportional term is added so block diagram of adaptive mechanism for evaluation of rotor speed has ultimate form presented in Fig. 1.

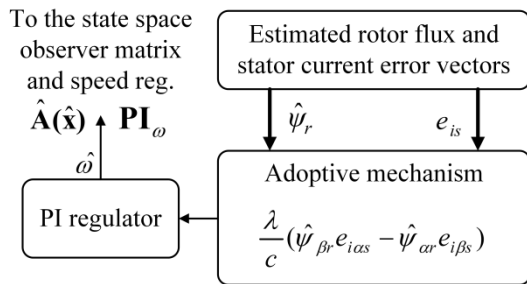


Figure 1. Adaptive mechanism for rotor speed estimation of IM

Finally, block diagram of complete LO for observation of unknown states of IM and estimation of rotor speed is represented in Fig. 2.

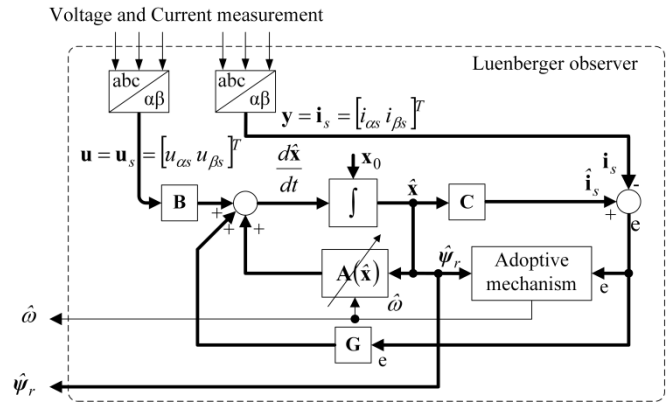


Figure 2. Block diagram of proposed LO for observation of unknown IM states and rotor speed

IV. DSP IMPLEMENTATION OF LUENBERGER OBSERVER FOR INDUCTION MOTOR

VU concept of IM control and various complicated algorithms for estimation and observation within IM drives requires exclusively DSC-based systems for quality control implementation. Those systems implement the algorithm law in discrete-time sequences. Due to that, it is of crucial importance to discretize the continuous model (14) in the meaning of magnitude and time discretization methodology. Also, *real time* applications requires execution of control law in limited-time sequences so model normalization is required for the purposes of utilization of *fixed-point* calculation method that saves, in the most occasions critical, CPU time.

First step for DSC realization of LO algorithm involves the method for normalization of state and control variables of IM. In case of a DSC implemented control of IM it is the most common practice to choose base state values to have maximum values which can appear in operation mode of IM drive. Motive for this comes from the fact that the problem of DSC registers saturation is then overcome.

Next step involves time discretization where the most common approach is based on approximation method which implies the substitution of complex s variable with complex z variable of relevant system represented in complex plane. For simplicity, it is often used *Forward Euler* approximation of complex s variable with z variable in the form of

$$s \rightarrow (z-1)/T \quad (24)$$

where T represents sample period which matches the PWM rate period. In the case of simulation and experiments of considered drive described in the next section, value of sample period correspond to the PWM frequency of 8 kHz. Therefore

$$T = T_{pwm} = 125 \mu s. \quad (25)$$

Third and final step of adapting the model (14) for DSC realization is based on magnitude discretization problem. Analog-to-Digital DSC unit automatically converts analog signal to digital.

Applying these three steps into LO continuous model (14) in complex plane (time derivation of state vector is substituted with complex variable s), discrete equations are obtained like:

$$\mathbf{i}_s^*(kT) = A_{r11}\mathbf{i}_s^*(kT - T) + (A_{r12} - jA_{i12}\omega_r^*)\boldsymbol{\psi}_r^*(kT - T) + B_r\mathbf{u}_s^*(kT - T) + T(\mathbf{g}_1^* + j\mathbf{g}_2^*)(\hat{\mathbf{i}}_s^*(kT - T) - \mathbf{i}_s^*(kT - T)) \quad (26)$$

$$\boldsymbol{\psi}_r^*(kT) = [A_{r22} + jA_{i22}\omega_r^*]\boldsymbol{\psi}_r^*(kT - T) + A_{r21}\mathbf{i}_s^*(kT - T) + T(\mathbf{g}_3^* + j\mathbf{g}_4^*)(\hat{\mathbf{i}}_s^*(kT - T) - \mathbf{i}_s^*(kT - T)) \quad (27)$$

where $A_{r11} = 1 - \omega_b T \left(\frac{r_s}{l_\sigma} + \frac{l_m^2 r_r}{l_r^2 l_\sigma} \right)$, $A_{r12} = \omega_b T \frac{l_m r_r}{l_r l_\sigma} \frac{1}{l_\sigma}$, $A_{i12} = \omega_{b1} T \frac{l_m}{l_r l_\sigma}$, $A_{r21} = \omega_b T r_r \frac{l_m}{l_r}$, and $A_{r22} = 1 - \omega_b T \frac{r_r}{l_r}$.

For calculation of (26) and (27) it is necessary to determine the values of motor parameters. One of the basic ways for extracting the parameter values from IM is through IM experiment at no-load and short-circuit state, [2].

In Table I parameter values of used IM are shown.

TABLE I. IM PARAMETER VALUES

R_s [Ω]	R_r [Ω]	L_s [H]	L_r [H]	L_m [H]
3.26	1.05	0.078	0.078	0.074

V. SYSTEM CONFIGURATION

Whirlpool three-phase IM (Maytag Whirlpool Factory Washer Motor W10171902 J58GTC-1132) is controlled via DSC MC56F8245 of FreeScale manufacturer which generates pulses with variable filling factor (PWM-pulse width modulated) to "GATE DRIVER" block that drives inverter. Vector control algorithm is implemented in DSC module. Measured variables are stator current from shunt in inverter DC circuitry and rotor shaft speed from tachogenerator. In case of LO, reconstructed stator currents are used for feedback action and utilized in adaptive mechanism for estimation of rotor speed. In that case, measured rotor speed serves only for system monitoring purposes. Interface between the user and drive system is, in the manner of programmability and control management sense, implemented through serial link. Fig. 3 represents simplified block diagram of digital VU IM sensorless drive.

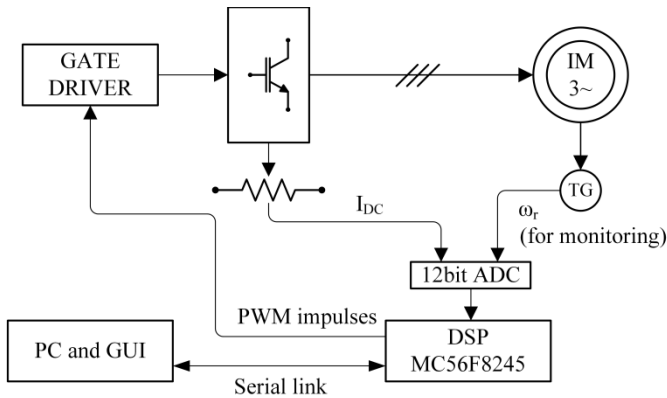


Figure 3. Simplified block diagram of IM drive

VI. SIMULATION AND EXPERIMENT

A. Simulation analysis of induction motor drive

Simulation analysis of LO algorithm performance within considered drive from Fig. 3. were implemented in *Simulink tool* of MATLAB software. Estimation results within basic observer modes such as open-loop and closed-loop modes were presented as well as the influence in discrete calculation methodology. Simulation analysis were performed at no-load condition of considered IM.

Observation responses of IM and continuous LO states in open-loop mode (pure rotor flux observer where rotor speed is measured and used from sensor) are presented in Figs. 4 and 5 at rotor speed references of 500 rpm and 2500 rpm.

From Figs. 4 and 5 it is noticeable the match of corresponding $\alpha\beta$ components of IM and LO states. From subplots in Figs. 4 and 5, blue- (correspond to $i_{s\alpha}^*$ from upper and $\psi_{s\alpha}^*$ from lower subplot) and green- (correspond to $i_{s\beta}^*$ from upper and $\psi_{s\beta}^*$ from lower subplot) colored graph components coincide the corresponding red- (correspond to $i_{s\alpha}$ from upper and $\psi_{s\alpha}$ from lower subplot) and yellow- (correspond to $i_{s\beta}$ from upper and $\psi_{s\beta}$ from lower subplot) dotted graph components. States with * represents observed states from LO.

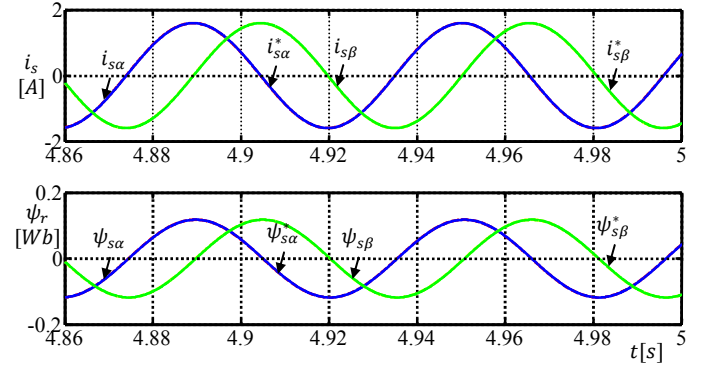


Figure 4. Current (upper subplot) and flux (lower subplot) responses of IM and continuous open-loop LO in $\alpha\beta$ frame, speed reference 500 rpm

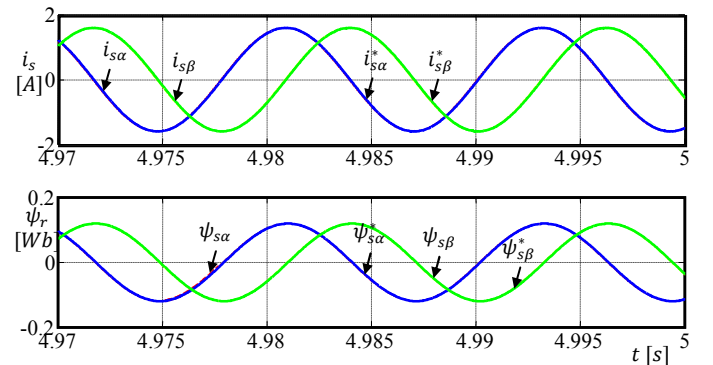


Figure 5. Current (upper subplot) and flux (lower subplot) responses of IM and continuous open-loop LO in $\alpha\beta$ frame, speed reference 2500 rpm

Observation responses of IM and discrete LO states in open-loop mode (rotor flux and speed observer where rotor speed is evaluated from adaptive mechanism, Fig. 1) are shown

in Figs. 6 and 7 at rotor speed references of 500 rpm and 2500 rpm, respectively.

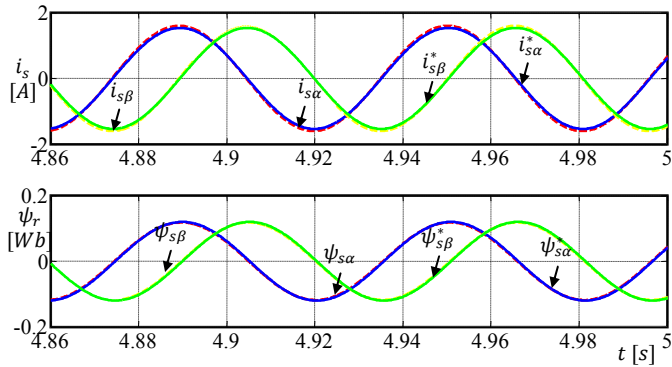


Figure 6. Current (upper subplot) and flux (lower subplot) responses of IM and discrete open-loop LO in $\alpha\beta$ frame, speed reference 500 rpm

Comparison of responses from Figs. 6 and 7 to the responses from Figs. 4 and 5 at identical simulation conditions shows bad influence of discrete calculation approximation method based on (24) to the observation of IM states. Proper magnitude as well as the phase loss of LO states particularly noticeable at higher speed reference values are repercussions from discrete equation utilization (26)–(27) within LO algorithm.

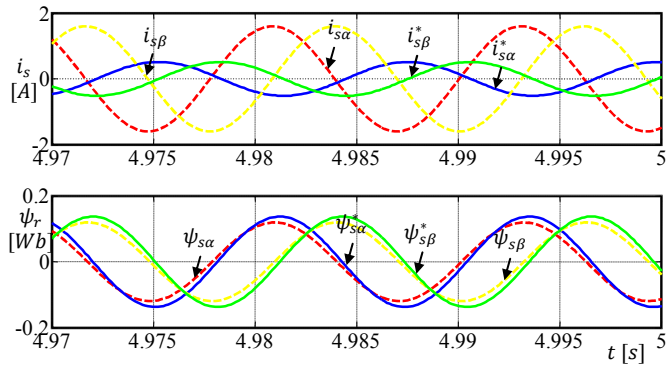


Figure 7. Current (upper subplot) and flux (lower subplot) responses of IM and discrete open-loop LO in $\alpha\beta$ frame, speed reference 2500 rpm

Responses of discrete LO states at closed-loop mode are similar to those at open-loop mode.

One of the solution for fixing the problem of magnitude and phase loss of LO state includes the use of feedback action within LO via stator current vector error.

Feedback action within LO inquires the use of non-zero gains of feedback action matrix G. If coefficient k from (16) is set on the value which differs from one than feedback is included in LO algorithm. It is often convenient to select this value to be greater than one mainly because the observation response converges faster to the stationary state of observation system.

Figs. 8 and 9 represents the observation responses of IM and discrete LO states in open- and closed-loop modes of LO algorithm with implemented feedback action at rotor speed reference of 2500 rpm, respectively.

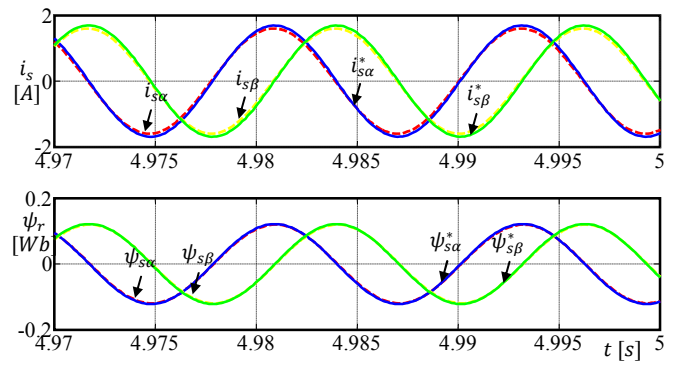


Figure 8. Current (upper subplot) and flux (lower subplot) responses of IM and discrete open-loop LO in $\alpha\beta$ frame with implemented feedback action $k = 3$, speed reference 2500 rpm

It is obvious from previous Fig. that the implementation of feedback within LO algorithm greatly reduces the magnitude and phase error between IM and observed LO states. In closed-loop mode coefficient k from (16) is set at value smaller than one, $k = 0.5$, because of stability issue disruption problem.

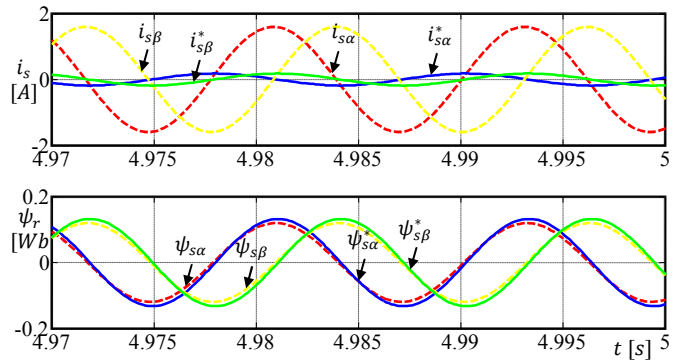


Figure 9. Current (upper subplot) and flux (lower subplot) responses of IM and discrete closed-loop LO in $\alpha\beta$ frame with implemented feedback action $k = 0.5$, speed reference 2500 rpm

Compare to the Fig. 7, it is clear from Fig. 9 that feedback action decrease the estimation error of observable states due to IM states but, compare to the Fig. 8 this correction has much smaller effect. Main reason lies in fact that feedback action matrix gains (17)–(20) are rotor speed-dependent. Rotor speed signal is estimated from adaptive mechanism (23). Discrete LO calculation method based on LE approximation has an inherent problem due to the appearance of observation error. Such erroneous states are utilized in adaptive mechanism and the aftermath is the inaccuracy of estimated speed signal (see Fig. 10.) and error accumulation problem in observation algorithm. Drawback of gain selection method based at (17)–(20) in closed-loop mode of LO is that the observer feedback action cannot drive the observation error to zero which affects the dynamic performance response and also stability in *sensorless* drives especially at high speed region.

Fig. 10 represents the rotor speed response from IM and adaptive mechanism implemented within LO (upper subplot) and also zoomed to the steady state condition (lower subplot), rotor speed reference value 2500 rpm. PI regulator gains

within adaptive mechanism were set at values $k_p = 30$ and $k_i = 60$.

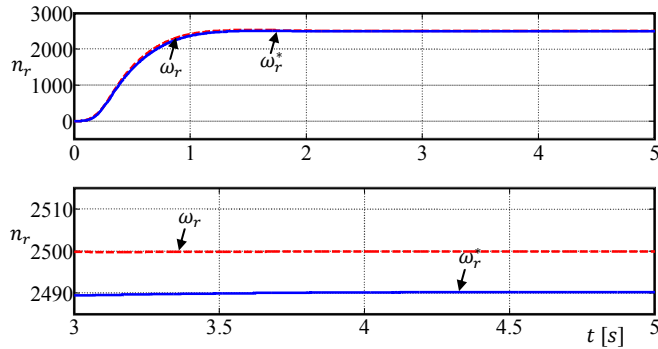


Figure 10. Speed responses from IM and adaptive mechanism within LO (upper subplot) and zoomed to the steady state conditions (lower subplot), speed reference 2500 rpm

B. Experimental analysis of induction motor drive

Validation of examined simulation results is given through appropriate experimental tests on subscribed IM drive, section V. Analysis are carried at identical no-load conditions of IM drive like in case of simulation tests.

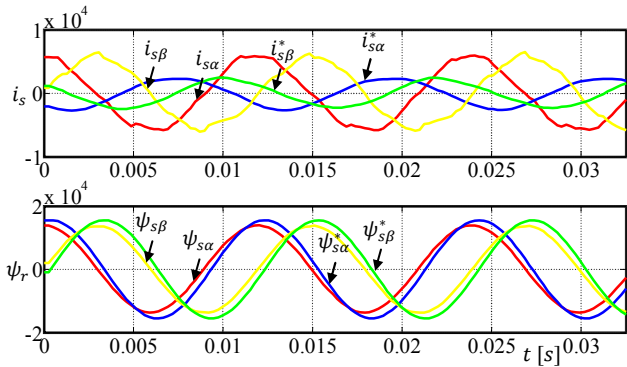


Figure 11. Current (upper subplot) and flux (lower subplot) responses of IM and discrete closed-loop LO in $\alpha\beta$ frame, speed reference 2500 rpm

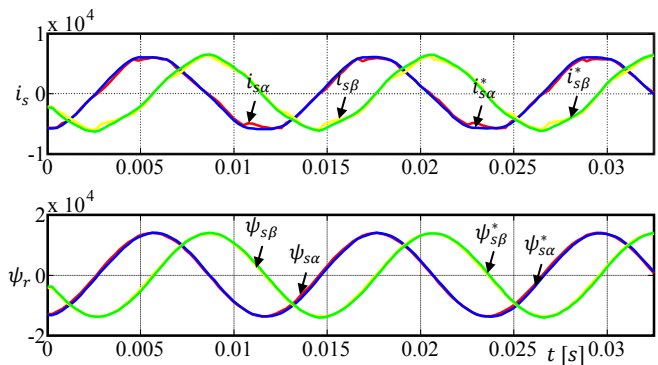


Figure 12. Current (upper subplot) and flux (lower subplot) responses of IM and discrete open-loop LO in $\alpha\beta$ frame, speed reference 2500 rpm

Fig. 11 shows the experimental responses of stator current and rotor flux of IM and discrete closed-loop LO at speed reference 2500 rpm. It should be advised that IM flux is derived from MRAS estimator which is also performed in

specified software for control management of considered drive. States with * represents observed states from LO. All variables from Fig. 11 are in relative domain and represented as fixed-point variables like in DSP registers.

The similar behavior at identical operating conditions is obvious from Figs. 7 and 11. The same statement valid at open loop mode of LO with feedback action $k = 3$. Fig. 12 confirms that conclusion.

Feedback action in closed-loop mode was not implemented because of critical stability issue of considered system.

VII. CONCLUSION

Performance evaluation of LO based *sensorless* method for IM is introduced in this paper. It is shown that discrete calculation method based on (24) and performed within LO algorithm has dominant effect on the accuracy of IM state and rotor speed observation. Drawback of the LO model approximate implementation algorithm (26)–(27) is the occurrence of degradation in both magnitude and phase of LO states to the IM states with greater effect at high speed region. Proposed method which includes the use of feedback law within LO is proven to be suitable in open-loop mode. Therefore, LO can be used as robust flux observer for IM drive performance improvements because it cancels bad effect of loss in magnitude and phase of observed LO states due to the IM states. In closed-loop mode where rotor speed is estimated in addition to the observed states, it is proven that feedback action did not cancel this effect. Actually small improvements in observation are conducted in that case and that is the main reason why this construction of LO is not suitable for appliance in high performance IM drives at wide speed range. Finally, the significant similarity is shown between simulation and experiment tests of considered IM drive.

REFERENCES

- [1] J. Holtz, "Sensorless control of induction machines-with or without signal injection," IEEE Trans. Ind. Electron., Vol. 53, No. 1, pp. 7–30, February 2006.
- [2] C. Schauder, "Adaptive speed identification for vector control of induction motors without rotational transducers," IEEE Trans. Ind. Appl., Vol. 28, No. 5, pp. 1054–1061, September/October 1992.
- [3] J. Maes and J. Melkebeek, "Speed sensorless direct torque control of induction motors using an adaptive flux observer," IEEE Trans. Ind. Appl., Vol. 36, No. 3, pp. 778–785, January 2000.
- [4] H. Rehman, A. Derdiyok, M. K. Güven and L. Xu, "A new current model flux observer for wide speed range sensorless control of an induction machine," IEEE Trans. Power Electron., Vol. 17, No. 6, pp. 1041–1048, June 2002.
- [5] H. Kubota, K. Matsuse and T. Nakano, "DSP-based speed adaptive flux observer for induction motor," IEEE Trans. Ind. Appl., Vol. 29, No. 2, pp. 344–348, March/April 1993.
- [6] Z. Yongchang and Z. Zhengming, "Speed Sensorless Control for Three-Level Inverter-Fed Induction Motors Using an Extended Luenberger Observer," IEEE Veh. Pow. Prop. Conf. (VPPC), September 3-5, 2008, Harbin, China
- [7] D. G. Luenberger, "An introduction to observers," IEEE Trans. Aut. Cont., Vol. AC-16, No. 6, pp. 596–602, December 1971.
- [8] S. N. Vukosavic, "Elektricne masine," Elektrotehnicki fakultet, Beograd, 2010.
- [9] D. P. Marcetic, "Mikroprocesorsko upravljanje energetskim pretvaracima," FTN Novi Sad, 2012.